Electrochimica Acta 54 (2009) 7042–7047

Contents lists available at ScienceDirect

Electrochimica Acta

journal homepage: www.elsevier.com/locate/electacta

Electrocatalytic properties of Pt/carbon composite nanofibers

Zhan Lin, Liwen Ji, Xiangwu Zhang*

Fiber and Polymer Science Program, Department of Textile Engineering, Chemistry and Science, North Carolina State University, 2401 Research Drive, Raleigh, NC 27695-8301, USA

ARTICLE INFO

Article history:
Received 12 May 2009
Received in revised form 6 July 2009
Accepted 7 July 2009
Available online 16 July 2009

Keywords:
Electrospinning
Electrodeposition
Pt nanoparticles
Carbon nanofibers
Methanol

ABSTRACT

Pt/carbon composite nanofibers were prepared by electrodepositing Pt nanoparticles directly onto electrospun carbon nanofibers. The morphology and size of Pt nanoparticles were controlled by the electrodeposition time. The resulting Pt/carbon composite nanofibers were characterized by running cyclic voltammograms in 0.20 M H_2SO_4 and 5.0 mM $K_4[Fe(CN)_6]$ + 0.10 M KCl solutions. The electrocatalytic activities of Pt/carbon composite nanofibers were measured by the oxidation of methanol. Results show that Pt/carbon composite nanofibers possess the properties of high active surface area and fast electron transfer rate, which lead to a good performance towards the electrocatalytic oxidation of methanol. It is also found that the Pt/carbon nanofiber electrode with a Pt loading of 0.170 mg cm^{-2} has the highest activity.

1. Introduction

Nanomaterials have received growing interest due to their unique chemical and physical properties according to their sizes and shapes [1]. Nanostructured carbons with different forms, such as fullerenes, nanotubes, and nanofibers, have fascinating structures and thermal/electric/mechanical properties, and hence they gained much attention due to their potential applications in diverse areas, ranging from fuel cells, supercapacitor, hydrogen storage, field emission devices, to chemical/biological sensors [2–10]. In many of these applications, the deposition of precious metallic or alloyed catalysts onto the carbon substrate is necessary to provide such desired functionalities as the electrocatalytic activity. In these cases, the structure and properties of the supporting carbon materials are crucial because they have significant impact on the size, distribution, and activity of the supported catalysts. For example, in direct methanol fuel cells, the methanol oxidation reaction (MOR) in acidic solution, typically catalyzed by Pt or its alloy, can be expressed in the following equation [11]:

$$CH_3OH + H_2O \rightarrow CO_2 + 6H^+ + 6e^-$$

$$E^0(\mathrm{MOR}) = 0.016\,\mathrm{V\ vs.\ SHE\ at\ 25\ ^\circ C}$$

For the reaction to happen, the catalyst particles must have simultaneous exposure to the reactants, protons, and electrons. Therefore, the development of highly active electrode catalysts coupled with a suitable electrode structure for the oxidation of methanol is an important subject to attaining the high efficiency in direct methanol fuel cells.

Carbon nanomaterials are currently being considered as the catalyst supports in direct methanol fuel cells, because of their unique graphite properties combined with three-dimensional flexible structures. Among various carbon nanomaterials, one-dimensional nano-carbons, such as carbon nanotubes and carbon nanofibers, are considered as promising support materials for catalysts in direct methanol fuel cells, thanks to their unique structures, high electronic and thermal conductivities, and good electrochemical stability [12,13]. Compared with carbon nanotubes, carbon nanofibers are inexpensive and can be produced with various controlled structures at relatively high speeds. However, most current research focused on the deposition of noble metal such as Pt nanoparticles onto carbon nanotubes [8,9,14–18] and there are only few literature reports on utilizing carbon nanofibers as the catalyst support [19–21]. For example, Li et al., recently utilized the pulsed electrodeposition method to prepare Pt-deposited carbon nanofibers, but the resultant Pt particle sizes are relatively large (~150 nm) [20]. Here, we report the preparation and characterization of Pt/carbon composite nanofibers by electrodepositing Pt nanoparticles with smaller diameters onto carbon nanofibers.

2. Experimental

2.1. Chemicals and reagents

Polyacrylonitrile (PAN), *N*,*N*-dimethylformamide (DMF), chloroplatinic acid hydrate ($H_2PtCl_6{\cdot}xH_2O$), potassium hexacyanoferrate

* Corresponding author. Tel.: +1 919 515 6547; fax: +1 919 515 6532.
E-mail address: xiangwu_zhang@ncsu.edu (X. Zhang).

0013-4686/$ – see front matter © 2009 Elsevier Ltd. All rights reserved.
doi:10.1016/j.electacta.2009.07.022

(II) ($K_4[Fe(CN)_6]$), sulfuric acid (H_2SO_4) and methanol (CH_3OH) were purchased from Sigma–Aldrich, and they were used without further purification. Deionized water was used throughout.

2.2. Synthesis of carbon nanofibers

A DMF solution of 8 wt% PAN was prepared at 60 °C, with mechanical stirring for 3.0 h. The electrospinning was conducted using a Gamma ES40P-20W/DAM variable high voltage power supply under a voltage of 15 kV. Under high voltage, a polymer jet was ejected and accelerated toward the nanofiber collector, during which the solvent was rapidly evaporated. The electrospun PAN fibers were collected on an aluminum foil placed on the collector. These PAN nanofibers were first stabilized in an air atmosphere at 280 °C for 2.0 h at the heating rate 5.0 °C min^{-1}, and then carbonized at 700 °C for 1.0 h in nitrogen atmosphere at the heating rate 2.0 °C min^{-1}. The resulting carbon nanofibers were used as the working electrode in the electrodeposition of Pt nanoparticles.

2.3. Electrodeposition of Pt onto carbon nanofibers

First, carbon nanofibers were directly used as the working electrode and were cycled in 1.0 M H_2SO_4 solution between −0.70 and 1.20 V for 100 cycles at 50.0 mV s^{-1} to form oxidized carbon nanofibers. The electrodeposition of Pt particles was carried out by applying a potential of −0.2 V with different deposition durations on the oxidized carbon nanofibers in a 5.0 mM $H_2PtCl_6{\cdot}xH_2O$ + 1.0 M H_2SO_4 solution.

The structure of carbon and Pt/carbon nanofibers, which were deposited onto 200 mesh carbon-coated Cu grids, was evaluated using a Hitachi HF-2000 TEM at 200 kV. These carbon and Pt/carbon nanofibers were also examined using a JEOL JSM-6360LV FESEM at 15 kV.

2.4. Electrochemical properties of Pt/carbon nanofibers

The electrochemical measurements of Pt/carbon nanofibers were performed in a three-electrode cell at 25.0 °C on an AQ4 Gamry Reference 600 electrochemical workstation. The cell consisted of a working electrode (Pt/carbon nanofibers), a counter electrode (Pt wire), and a reference electrode (Ag/AgCl/4.0 M KCl). Nitrogen was used to bubble the testing solutions for at least 30 min before the measurements, and then was used continually to protect the experiment environment. All the electrochemical potentials were measured and reported with respect to Ag/AgCl/4.0 M KCl.

The measurement of hydrogen electrosorption was conducted by cyclic voltammograms (CVs) of Pt/carbon nanofiber electrodes in 0.50 M H_2SO_4 at 50.0 mV s^{-1} to determine the electrochemically active surface area (Ar/cm^2). The electron transfer properties were determined by CVs of Pt/carbon nanofibers in 5.0 mM $K_4[Fe(CN)_6]$ + 0.50 M KCl at 50.0 mV s^{-1}. CVs of Pt/carbon nanofibers in 0.125 M CH_3OH + 0.20 M H_2SO_4 at 5.0 mV s^{-1} were also carried out to study their activities on the methanol oxidation.

3. Results and discussion

3.1. Surface oxidation of carbon nanofibers in 1.0 M H_2SO_4

Fig. 1 shows the SEM image of carbon nanofibers before surface oxidation. It is shown that carbon nanofibers from PAN precursor have relatively smooth and regular surface morphology, with fiber diameters ranging from 200 to 300 nm. The fiber diameters can be further reduced by manipulating spinning voltage, solution concentration, solvent type, and other processing parameters. Typically, smaller fiber diameter benefits the electrodeposition of Pt nanoparticles due to increased accessible surface area.

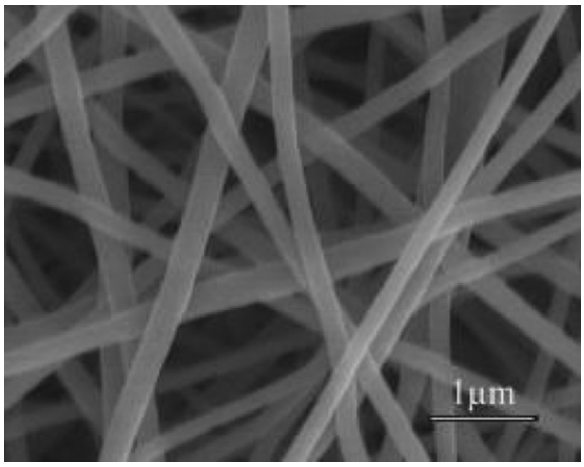

Fig. 1. SEM image of carbon nanofibers before surface oxidation.

In order to carry out the surface oxidation, carbon nanofibers were used as the working electrode and were cycled in 1.0 M H_2SO_4 at different scan rates using CVs, and the results are shown in Fig. 2. It is seen that two current peaks are found at ±0.48 V, respectively, and they can be attributable to the redox reactions of surface functional groups such as quinoid [5]. Moreover, the current density increases with increase in scan rate. The response of the anodic current density peak (I_{pa}) was measured as a function of scan rate and is shown in the inset of Fig. 2. I_{pa} depends almost linearly upon the scan rate, which is due to the Faradic process occurring on the surface of carbon nanofibers.

3.2. TEM images of carbon and Pt/carbon nanofibers

After the surface oxidation, Pt particles were electrodeposited onto the carbon nanofiber surface. Fig. 3 shows TEM images of carbon nanofibers and Pt/carbon composite nanofibers with 1.0 h deposition time. It is seen that before electrodeposition, the carbon nanofiber surface is smooth and there are no particles loaded. However, Pt nanoparticles are evenly distributed on the surface of carbon nanofibers after the electrodeposition. The typical particle diameters are around 20 nm and they are smaller than those reported by some literature, in which a pulsed electrodeposition method was used [20,21]. Fig. 3d shows the energy dispersive X-ray spectroscopy (EDS) of Pt/carbon nanofibers. The EDS curve

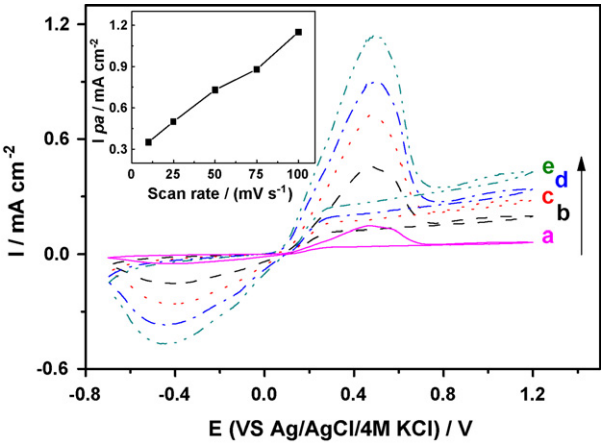

Fig. 2. Surface oxidation of carbon nanofibers in 1.0 M H_2SO_4 at the scan rate of (a) 10.0, (b) 25.0, (c) 50.0, (d) 75.0, and (e) 100.0 mV s^{-1}. The relationship between anodic peak current (I_{pa}) and scan rate is shown in the inset.

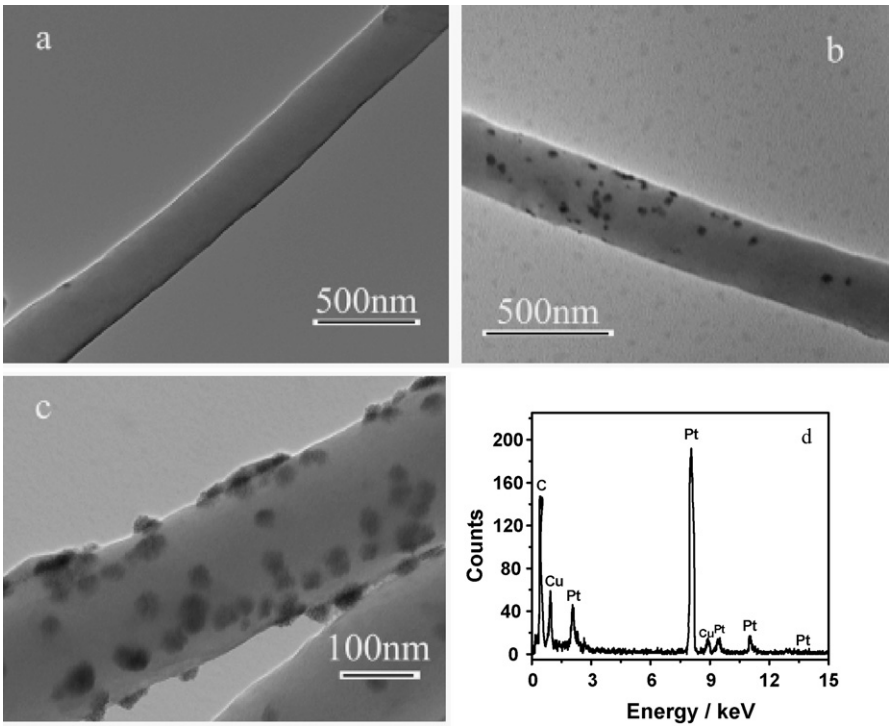

Fig. 3. TEM images of carbon (a), Pt/carbon (b and c) nanofibers, and EDS spectrum of Pt/carbon nanofibers (d). Deposition time: 1.0 h.

also confirms the presence of Pt particles on the surface of carbon nanofibers. The Cu peak in Fig. 3d belongs to the TEM grid background.

3.3. SEM images of Pt/carbon nanofibers

The amount (m_{Pt}) of Pt loading can be calculated by the following equation:

$$m_{Pt} = \frac{Q_{Pt}M}{4FS} \quad (1)$$

where M is the atomic weight of Pt (195.09 g mol^{-1}), Q_{Pt} the electrons transferred (C), S the geometric area of carbon nanofiber electrode (cm^{-2}), and F the Faraday constant (96485 C mol^{-1}). In this work, four different deposition durations of 0.5, 1.0, 2.0, and 3.0 h were used, and the Pt loadings of the resultant Pt/carbon nanofibers are 0.085, 0.170, 0.335, and 0.545 mg cm^{-2}, respectively. Fig. 4a–d shows SEM images of these Pt/carbon composite nanofibers. When the deposition time is 0.5 h, the resultant Pt loading of 0.085 mg cm^{-2} is relatively low, and hence Pt nanoparticles cannot be visually seen on the surface of carbon nanofibers. However, the electrochemical measurements discussed in the following sections show the presence of Pt nanoparticles on carbon nanofibers at this low loading. When the deposition time is beyond 0.5 h, well-distributed Pt nanoparticles can be observed on the surface of carbon nanofibers. Moreover, with increase in deposition time, the surface morphology of carbon nanofibers becomes rougher and the diameter of Pt nanoparticles increases. That is because the application of a longer deposition time results in higher Pt nanoparticle loading without increasing the quantity of nuclei. As a result, with increase in deposition time (i.e., Pt loading), the Pt nanoparticle size increases.

Fig. 4a–d only shows Pt nanoparticles deposited on the outer nanofiber layers. In order to ensure that nanoparticles have been deposited onto the surface of deeper layers, a SEM image was taken after mechanically peeling off three layers of Pt/carbon composite nanofibers (Fig. 4e). It is seen that Pt nanoparticles are distributed on the nanofiber surface, indicating that Pt ions can penetrate deep into carbon nanofiber layers during electrodeposition and be reduced to Pt nanoparticles.

3.4. Electrochemical characterization of Pt/carbon nanofibers

CV measurements of carbon and Pt/carbon nanofibers between −0.25 and +0.30 V at 50.0 mV s^{-1} in 0.20 M H_2SO_4 were employed to examine whether Pt particles on carbon nanofiber surface are electrochemically active (Fig. 5). It is seen that there is no redox peak found in carbon nanofibers, indicating no electrochemical activity. However, after the electrochemical deposition of Pt particles, redox current density peaks were observed. These redox peaks are due to the adsorption and desorption of hydrogen at the surface of Pt particles on carbon nanofibers. Moreover, the integration of CV curves after correcting for the double layer charging gives the quantities of charge, Q_H (μC), which are shown in Table 1. According to the theoretical value of electricity $Q_H^0 = 210$ μC per real cm^2 of Pt [22], the electrochemically active surface areas of Pt/carbon nanofibers can be estimated from $Ar = Q_H/Q_H^0$, which are also shown in Table 1. From Table 1, it is found that with increase in deposition time, the Pt electroactive surface area increases.

In order to study the electron transfer properties of carbon nanofibers before and after Pt particle deposition, steady-stated CV experiments were carried out at 50.0 mV s^{-1} in 5.0 mM $K_4[Fe(CN)_6]$ + 1.0 M KCl, in which $K_4[Fe(CN)_6]$ served as a probe for the fast electron transfer (Fig. 6). A pair of well-defined redox peaks for $Fe(CN)_6^{3-}/Fe(CN)_6^{4-}$ are found in Pt/carbon nanofibers at E = −0.12 and 0.04 V, respectively, indicating that

Table 1
Charge quantities and electrochemically active surface areas of Pt/carbon nanofibers with different deposition durations. Solution: 0.20 M H_2SO_4. Scanning rate: 50.0 mV s^{-1}.

Deposition duration (h)	0.5	1.0	2.0	3.0
Q_H (μC)	77.3	92.7	122.8	187.0
Ar (cm^2)	0.37	0.44	0.58	0.89

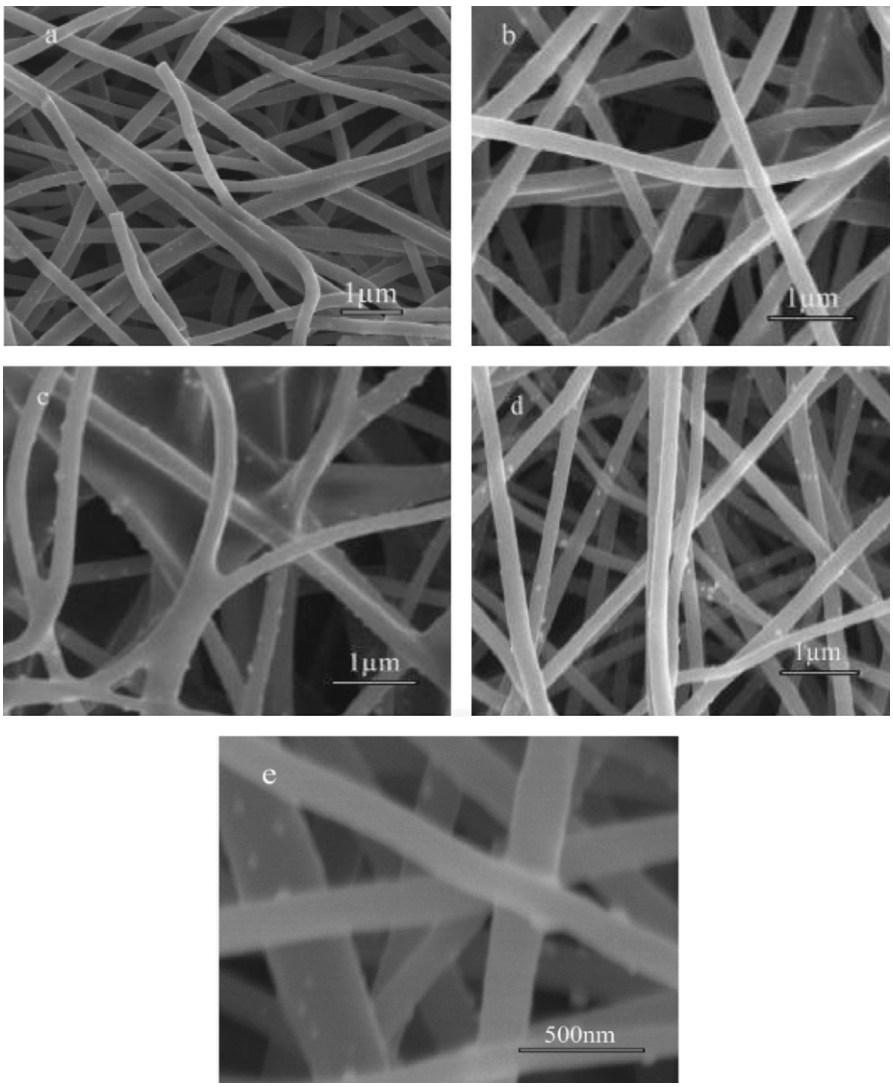

Fig. 4. SEM images of Pt/carbon nanofibers prepared using different deposition durations (a: 0.5, b: 1.0, c: 2.0, d: 3.0, and e: 3.0 h).

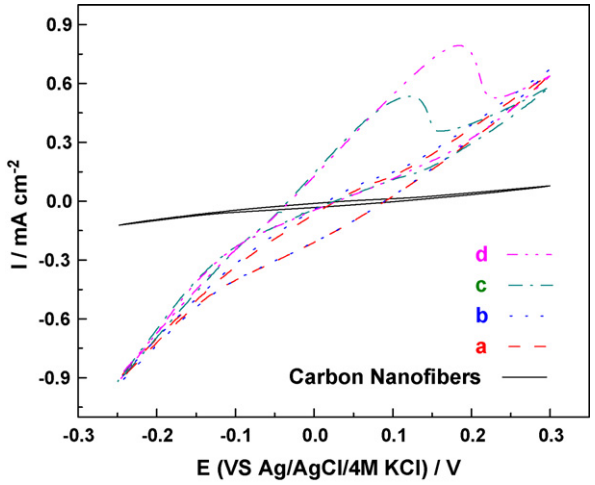

Fig. 5. CV responses in 0.2 M H_2SO_4 for carbon and Pt/carbon nanofibers prepared using different deposition durations (a: 0.5, b: 1.0, c: 2.0, and d: 3.0 h). Scanning rate: 50.0 mV s^{-1}.

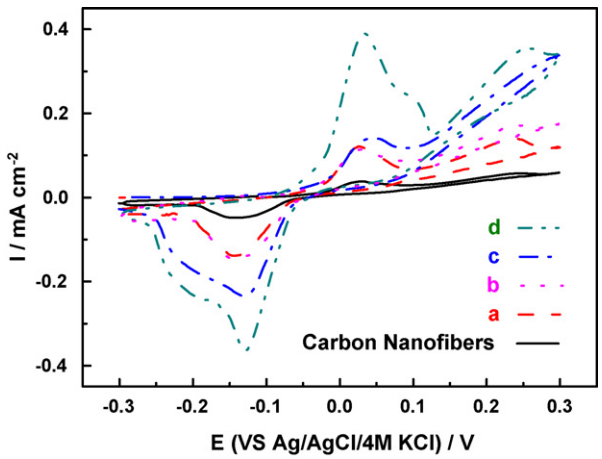

Fig. 6. CV responses in 5.0 mM $K_4[Fe(CN)_6]$ + 0.1 M KCl for carbon and Pt/carbon nanofibers prepared using different deposition durations (a: 0.5, b: 1.0, c: 2.0, and d: 3.0 h). Scanning rate: 50.0 mV s^{-1}.

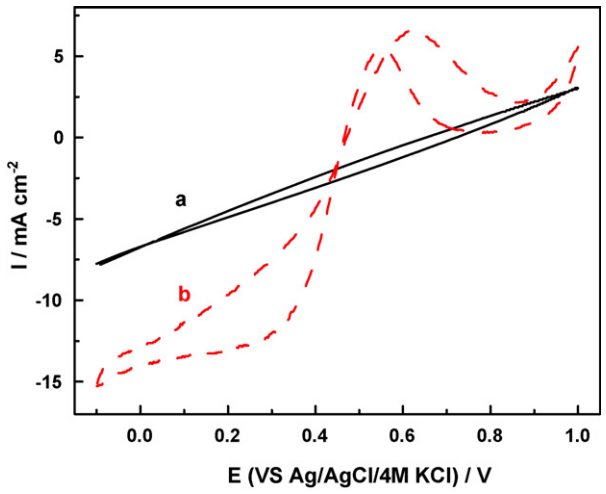

Fig. 7. Current–potential curves of carbon (a) and Pt/carbon (b) in 0.125 M CH_3OH + 0.20 M H_2SO_4 at 5.0 mV s^{-1}. Deposition time: 1.0 h.

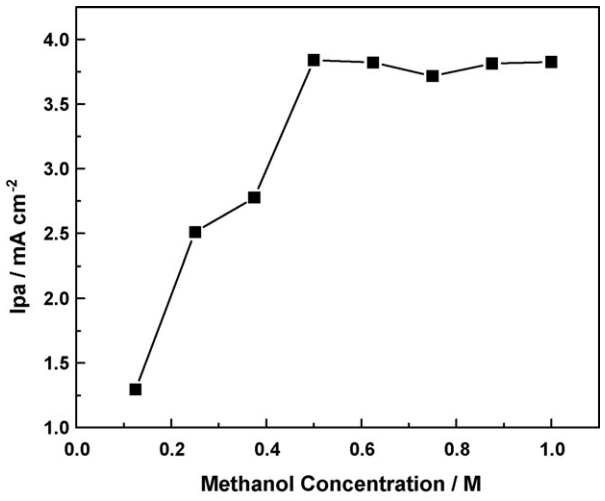

Fig. 8. Anodic peak current as a functional of methanol concentration for Pt/carbon nanofibers in 0.50 M CH_3OH + 0.20 M H_2SO_4 at 5.0 mV s^{-1}. Deposition time: 1.0 h.

Pt/carbon nanofibers have fast electron transfer kinetics, which may be due to the high electric conductivity and fascinating three-dimensional structures of these nanofibers [23].

3.5. Electro-oxidation of methanol on Pt/carbon nanofibers

Fig. 7 shows the current density–potential curves of carbon and Pt/carbon nanofibers in 0.125 M CH_3OH + 0.20 M H_2SO_4 solution at 5.0 mV s^{-1}. There is no methanol oxidation peak found for carbon nanofibers. In comparison, Pt/carbon nanofibers present a relatively large methanol electro-oxidation peak, which starts at +0.40 V with a maximum current peak +0.62 V. After the maximum, a decrease in current is observed due to the formation of oxides on the Pt surface, which decreases the number of active sites. Moreover, another current density peak is found at +0.55 V, which signifies the desorption of CO generated during the methanol oxidation [9].

In order to study the efficiency of methanol oxidation, the electrochemical characteristic data of Pt/carbon nanofibers with different deposition durations are summarized in Table 2. The efficiencies of methanol oxidation were compared in items of forward peak potential, forward peak current density (I_{pa}), and the mass activity (peak current density of methanol oxidation per unit of Pt loading [7]). From Table 2, it is seen that with increase in Pt loading, the forward peak current density increases due to increased amount of available Pt catalyst. With increase in Pt loading, the mass activity increases first and then reaches a maximum when the loading is 0.170 mg cm^{-2}, i.e., deposition time = 1.0 h. The existence of a maximum mass activity may be related to the size effect of Pt particles. When the Pt loading is higher than 0.170 mg cm^{-2}, the size of Pt particles become larger, which may play a role in reducing the mass activity of Pt/carbon nanofibers. In addition to the maximum mass activity, a minimum forward peak potential is obtained at the loading of 0.170 mg cm^{-2}, indicating that superior catalytic activity at that loading.

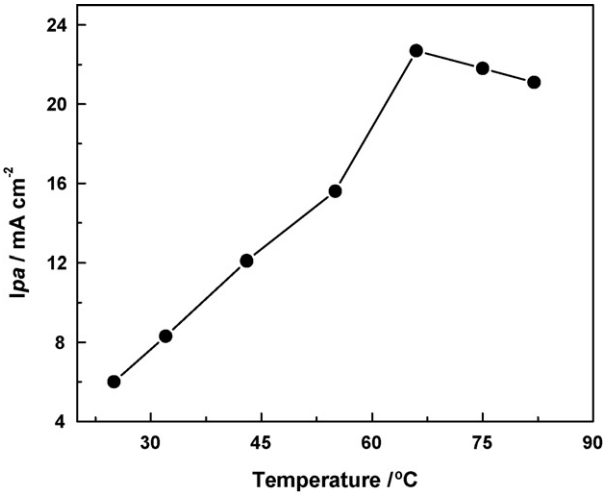

Fig. 9. Anodic peak current density as a function of solution temperature for Pt/carbon nanofibers in 0.50 M CH_3OH + 0.20 M H_2SO_4 at 5.0 mV s^{-1}. Deposition time: 1.0 h.

Fig. 8 shows the effect of methanol concentration on the anodic current density of Pt/carbon nanofibers during methanol oxidation. It is seen that, with increase in methanol concentration, the anodic current density increases first, but keeps relatively constant when the methanol concentration is greater than 0.50 M due to the saturation of Pt active sites at high methanol concentrations.

The effect of solution temperature on the anodic peak current density of Pt/carbon nanofibers during methanol oxidation is shown in Fig. 9. With increasing temperature, a linear increase in the anodic peak current is observed from 25.0 to 70.0 °C. After reaching 70.0 °C, the anodic peak current starts to decrease. The increase in the peak current density can be attributed to the acceleration of

Table 2
Electrochemical characteristics of Pt/carbon nanofibers with different deposition durations. Solution: 0.125 M CH_3OH + 0.20 M H_2SO_4. Scanning rate: 5.0 mV s^{-1}.

Deposition duration (h)	Catalyst loading (mg cm^{-2})	Forward peak potential (V vs. Ag/AgCl/4.0 M KCl)	Forward peak current density (I_{pa}, mA cm^{-2})	Mass activity ($A\ g^{-1}$)
0.5	0.085	+0.63	2.33	27.41
1.0	0.170	+0.62	6.55	38.53
2.0	0.335	+0.63	10.43	31.13
3.0	0.545	+0.65	12.67	23.24

the electrode reaction kinetics. At temperatures beyond 70 °C, the decrease in anodic peak is caused by the evaporation of methanol, which has a boiling point of 64.7 °C.

4. Conclusions

Pt/carbon nanofibers have been prepared by electrodepositing Pt nanoparticles onto electrospun carbon nanofibers under the potential −0.2 V. Particles with well-defined morphology and size were obtained by controlling the electrodeposition time. The deposition time can also be used to control the Pt loading and the catalyst activity. The resulting Pt/carbon nanofibers possess the properties of high active surface area and fast electron transfer rate, which lead to a good performance towards the electrocatalytic oxidation of methanol. The electrocatalytical activities of Pt/carbon nanofibers with different deposition times have been evaluated. The results show that the Pt/carbon electrode with suitable deposition time (1.0 h here) has the highest electrocatalytic activity. Therefore, the electrochemical deposition of Pt nanoparticles on carbon nanofibers provides an alternative method to obtain a good catalyst toward the oxidation of methanol. However, investigations into the catalytic ability of such composites in membrane electrode assembly in direct methanol fuel cells are needed for future applications.

Acknowledgements

This work was supported by the National Textile Center (ITA-08-07400), U.S. National Science Foundation (0833837), and ACS Petroleum Research Fund (47863-G10).

References

[1] Y.N. Xia, P.D. Yang, Y.G. Sun, Y.Y. Wu, B. Mayers, B. Gates, Y.D. Yin, F. Kim, Y.Q. Yan, Adv. Mater. 15 (2003) 353.
[2] A.S. Arico, P. Creti, N. Giordano, V. Antonucci, P.L. Antonucci, A. Chuvilin, J. Appl. Electrochem. 26 (1996) 959.
[3] C. Park, P.E. Anderson, A. Chambers, C.D. Tan, R. Hidalgo, N.M. Rodriguez, J. Phys. Chem. B 103 (1999) 10572.
[4] K.P. De Jong, J.W. Geus, Catal. Rev. Sci. Eng. 42 (2000) 481.
[5] J.H. Chen, W.Z. Li, D.Z. Wang, S.X. Yang, J.G. Wen, Z.F. Ren, Carbon 40 (2002) 1193.
[6] J.S. Yu, S. Kang, S.B. Yoon, G. Chai, J. Am. Chem. Soc. 124 (2002) 9382.
[7] H. Tang, J.H. Chen, L.H. Nie, D.Y. Liu, W. Deng, Y.F. Kuang, S.Z. Yao, J. Colloid Interface Sci. 269 (2004) 26.
[8] M.M.E. Duarte, A.S. Pilla, J.M. Sieben, C.E. Mayer, Electrochem. Commun. 8 (2006) 159.
[9] M.C. Tsai, T.K. Yeh, C.H. Tsai, Electrochem. Commun. 8 (2006) 1445.
[10] W.E. Billups, J. Am. Chem. Soc. (2008).
[11] N. Wakabayashi, H. Uchida, M. Watanabe, Electrochem. Solid State. 5 (2002) E62.
[12] G.L. Che, B.B. Lakshmi, E.R. Fisher, C.R. Martin, Nature 393 (1998) 346.
[13] S.H. Joo, S.J. Choi, I. Oh, J. Kwak, Z. Liu, O. Terasaki, R. Ryoo, Nature 412 (2001) 169.
[14] L. Cao, F. Scheib, C. Roth, F. Schweiger, C. Cremers, U. Stimming, H. Fuess, L. Chen, W. Zhu, X. Qiu, Angew. Chem. Int. Ed. 45 (2006) 5315.
[15] S. Hrapovic, Y.L. Liu, K.B. Male, J.H.T. Luong, Anal. Chem. 76 (2004) 1083.
[16] Z.Q. Tian, S.P. Jiang, Y.M. Liang, P.K. Shen, J. Phys. Chem. B 110 (2006) 5343.
[17] J.H. Ye, P.S. Fedkiw, Electrochim. Acta 41 (1996) 221.
[18] Z.B. He, J.H. Chen, D.Y. Liu, H. Tang, W. Deng, W.F. Kuang, Mater. Chem. Phys. 85 (2004) 396.
[19] J. Guo, G. Sun, Q. Wang, G. Wang, Z. Zhou, S. Tang, L. Jiang, B. Zhou, Q. Xin, Carbon 44 (2006) 152.
[20] M. Li, G. Han, B. Yang, Electrochem. Commun. 10 (2008) 880.
[21] M. Li, G. Han, B. Yang, J. Power Sources 191 (2009) 351.
[22] K. Shimazu, D. Weisshaar, T. Kuwana, J. Electroanal. Chem. 223 (1987) 223.
[23] J.S. Huang, D.W. Wang, H.Q. Hou, T.Y. You, Adv. Funct. Mater. 18 (2008) 441.